Int. J. Electrochem. Sci., 7 **(2012)** 760 - 767

International Journal of
ELECTROCHEMICAL
SCIENCE
www.electrochemsci.org

Synthesis and Characterization of Spherical-Like Tin-Nickel Alloy as Anode for Lithium Ion Batteries

Mi Lu[1,*], *Yanyan Tian*[2], *Youpeng Li*[1], *Wanlu Li*[1], *Xiaodong Zheng*[1], *Bing Huang*[1]

[1] Clean Energy Research and Development Center, Binzhou University, Binzhou, China, 256603
[2] Department of Chemistry, Xiamen University, Xiamen, China, 361005
[*]E-mail: lumihit@sina.com

Received: 15 September 2011 / *Accepted:* 24 November 2011 / *Published:* 1 January 2012

A kind of nanosized, spherical-like Sn-Ni alloy composite was synthesized by spray drying the ball-milled mixture of SnO_2, NiO and Super P carbon to obtain the precursor, then the metal oxides were reduced by carbon at 900 ℃ for 2 hrs. The morphology of the sample shown by scanning electronic spectroscopy was spherical-like particle with a diameter below 200 nm. X-ray diffraction pattern shows that the sample contains the alloy phase of Ni_3Sn_4, Ni_2Sn_2 and Ni_3Sn, element phase of Ni and Sn, and compound phase SnO_2. The charge/discharge test shows that the alloy shows a reversible capacity of 571.1mAh/g with capacity retention of 78.6% after 20 charge-discharge cycles. The improved performance was ascribed to the lower particle size, the higher contents of alloy phase, the binder styrene butadiene rubber to buffer the expansion of the alloy and the improved electric contact between active material and copper current collector.

Keywords: Lithium ion batteries; anode; alloy; Sn-Ni; composite

1. INTRODUCTION

Tin-based alloy anode for lithium ion batteries has attracted much attention due to its high theoretical specific capacity (994mAh g^{-1}), relative higher potential of lithium alloy formation and no solvent cointercalation [1]. But the changes of Sn-based anode in structure and in volume while alloying with lithium results the capacity rapidly fades with cycling. Several approaches have been developed including multiphase composites, particle size control, thin film and amorphous alloys etc.[2]. The tin based composite oxide (TCO) by the work of Fuji Photo Film Celltech first introduce the concept of electrochemically inactive matrix, which exhibits a very high specific charge of >600 mAh g^{-1} [1]. But TCO shows a very high irreversible capacity and its commercialization is unsuccessful. Real commercialization of Sn-based alloy was announced by Sony in 2005, who use the

Sn-Co-C alloy as anode and increased the capacity of its Nexelion battery by 30% [3]. The price of cobalt is high and the replacement of cobalt by nickel is a realistic option. The synthesis methods for Sn-Ni alloy include electroplating [4-8], ball-milling [9,10], carbothermal reduction [11,12], composite with graphite [13] or Al_2O_3 [14]. The electroplating generally results good electrochemical due to the thin of the active material and the performance can be further improved by porous structure [7]. But the electrode produced by electroplating encounters the barriers of scaling up and the problems during battery manufactures. From the application view, alloy powder anode may be advantage to the replacement of graphite anode due to similar manufacture process and equipments. Furthermore, the electrochemical performance of Sn-based alloy does not totally reach the requirement of lithium ion batteries, especially for its coulombic efficiency and cyclic stability. The mixture of alloy powder with graphite can improve the performance due to the graphite buffers the volume change of alloy during alloying with lithium [13], which makes the composite of Sn-based alloy and graphite is a realistic option for lithium ion batteries. Spray drying is a common method to obtain a controlled particle size and morphology precursor, which has been used to prepared spherical materials for lithium ion batteries [15-17]. In this paper, the oxides of tin and nickel with reductant carbon was mixed homogenously by ball-milling and spray drying, then heat treated at 900 ℃ to obtain Sn-Ni alloy and investigate its electrochemical performance.

2 EXPERIMENTAL PART

2.1 Synthesis of Sn-Ni alloy composite

The molar ration of the designed alloy was 1:1 and the stoichiometric nanosized SnO_2 (Aladdin, China, particle size about 50-70nm), spherical NiO (Aladdin, China, particle size about 30nm) and Super P (TIMCAL) carbon black was ball-milled at 200 rm/min for 15 hrs, then the ball-milled mixture was dispersed in a mixture of alcohol, deionized water dissolved with sucrose (sucrose content was 10 wt.% of the weight of the resulted alloy, the pyrolytic carbon content in the sample is about 2 wt.%), and small amount of Polyethylene glycol (PEG) to obtain an emulsion. Then the emulsion was stirred with magnetic stirring and spray dried at 130 ℃. The spray dried precursor was then heated to 900 ℃ at a heating rate of 5℃/min for 2 hrs under a mixture of argon/hydrogen (9:1 in volume) atmosphere.

2. 2 Physical characterization

The morphology of the sample was observed using a scanning electron microscope (SEM) (S4800, Hitachi, Japan) operating at 15 kV. The structure of the alloy was measured by X-ray diffraction (XRD) (X'pert PRO, Panalytical, Netherlands) with a CuKα radiation and a scanning rate of 10 deg./min in a range of 2θ values from 10-90^o and a step size of 0.02^o.

2.3 Electrochemical performance test

A slurry of alloy was prepared by ball-milling a mixture of 10 wt.% Super P (TIMCAL) carbon as conductive regent, 10 wt.% styrene butadiene rubber (SBR) together with 10 wt.% sodium carboxymethyl cellulose (CMC) as binder and an adequate amount of deionized water for 2 hrs. The slurry was coated onto a copper foil with an area of 1 cm^2 and then dried at 100 °C under vacuum (below -0.09) for more than 10 hrs to obtain an electrode for measurement. CR2025 coin-type cells were assembled in an argon-filled glove box (Etelux 2000, China), where both moisture and oxygen levels were kept at less than 1 ppm. $LiPF_6$ (1 mol/L) in ethylene carbonate and dimethyl carbonate (EC-DMC, 1:1 v/v) was used as the electrolyte and lithium foil was used as the counter electrode. Charge/discharge cycles were performed using a Neware® instrument (China) with a stable current of 0.1 C (based on the theoretical capacity of Sn-Ni alloy).

Electrochemical impedance spectroscopy was measured by a CHI 604 C electrochemistry workstation (Chenhua, China) in the frequency region of 100 k Hz-0.01 Hz. The cell was measured at the end of the first, second and the tenth discharge.

3. RESULTS AND DISCUSSION

The SEM of the prepared samples was shown in figure 1.

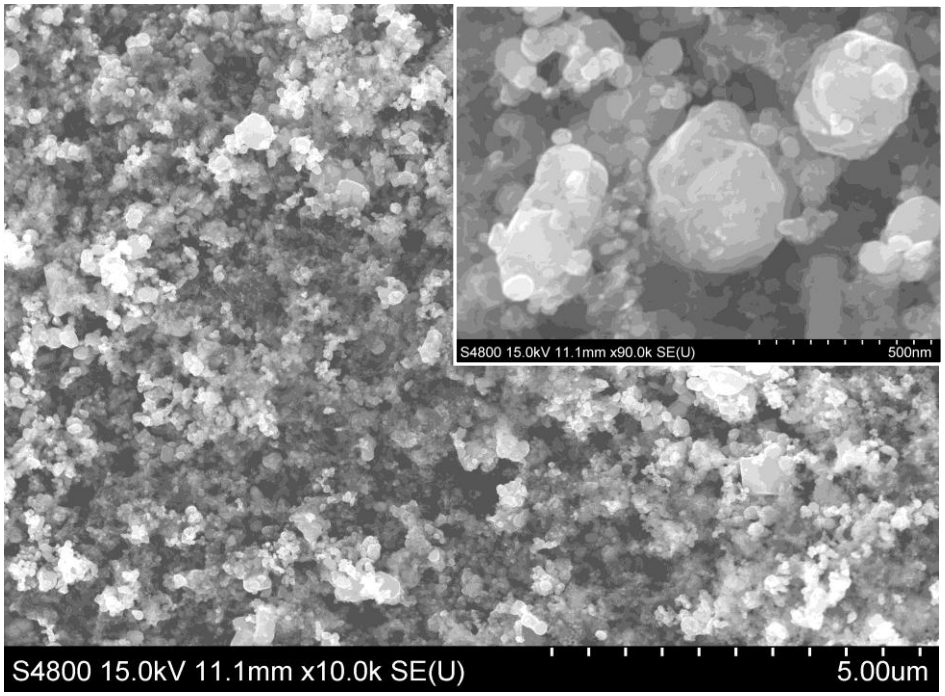

Figure 1. SEM of the Sn-Ni alloy composite. The inset was the magnified plot

The morphology showed that some big sphere-like particles with a diameter about 150-200 nm was dispersed in the smaller spherical-like particles with a diameter below 50 nm. It is generally accepted that the smaller size of the alloy is advantage to the cycling stability due to the expansion of the single particle is relative small [18]. Results showed that the adoption of nanosized raw materials is an effective way in controlling the particle size of the alloy. The sphere is easy to be formed due to the melting point of the reduced tin is only 232 ℃, and the liquid naturally forms spherical droplet to lower its surface energy and maintains the morphology during the cooling process. Thus, most of the reduced tin shows a spherical morphology [12]. For the sample prepared in this paper, the position of SnO_2 and NiO was fixed by sucrose during spray drying. The gathering of the nanosized products was suppressed by the carbon, thus the spherical morphology of the sample is irregular and the particle size is small.

The XRD pattern of the sample is shown in figure 2.

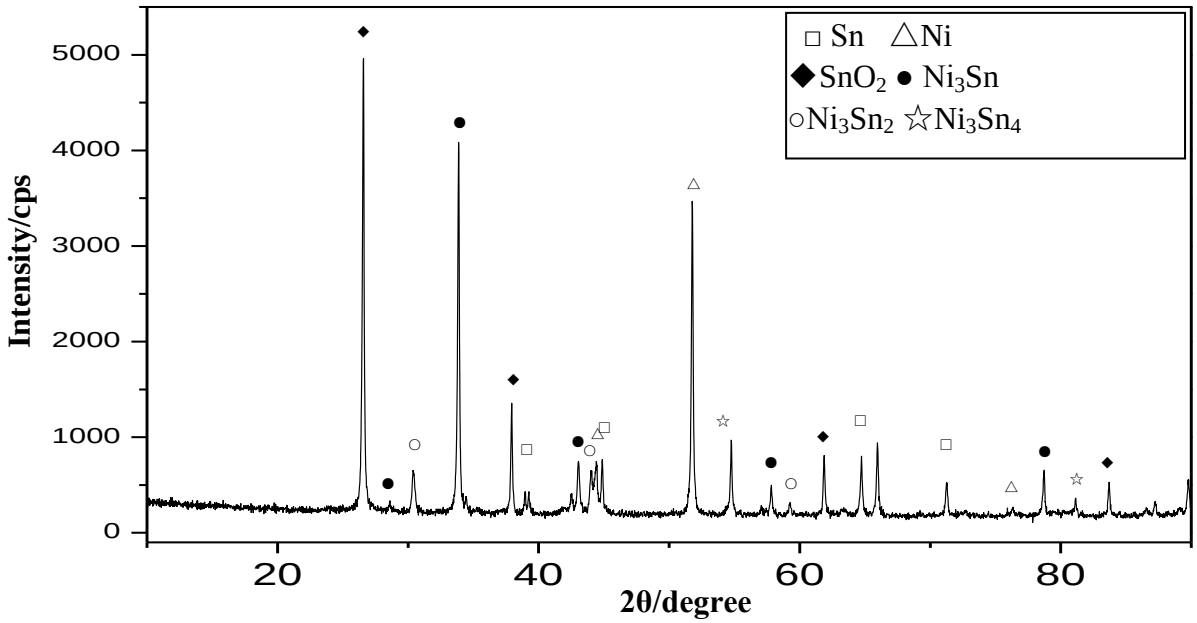

Figure 2. XRD of the Sn-Ni alloy composite

It showed a sharp peak at 26.58^o, corresponding to SnO_2. The residual peaks corresponding to the alloy phase of Ni_3Sn_4, Ni_3Sn_2 and Ni_3Sn, elemental phase of Ni and Sn [18-22]. The SnO_2, comes from the unreduced raw material or the reduced tin was oxidized during the exposure on the air, showing a theoretical lithium intercalation capacity about 780 mAh g^{-1}[23], did not affect the reversible capacity of the sample but the irreversible capacity was increased due to the formation of Li_2O and Sn during the lithium insertion process [24]. The elemental nickel and tin was formed due to the contactless of some reduced metal tin and nickel.

The charge-discharge profile is shown in figure 3. The discharge plot shows an obvious plateau at about 0.3V and then gradually decreased to the end potential. The relative higher lithium alloying

potential is advantage to avoid the lithium dendrite formation, thus be benefit to the improvement of the safety performance of lithium ion battery.

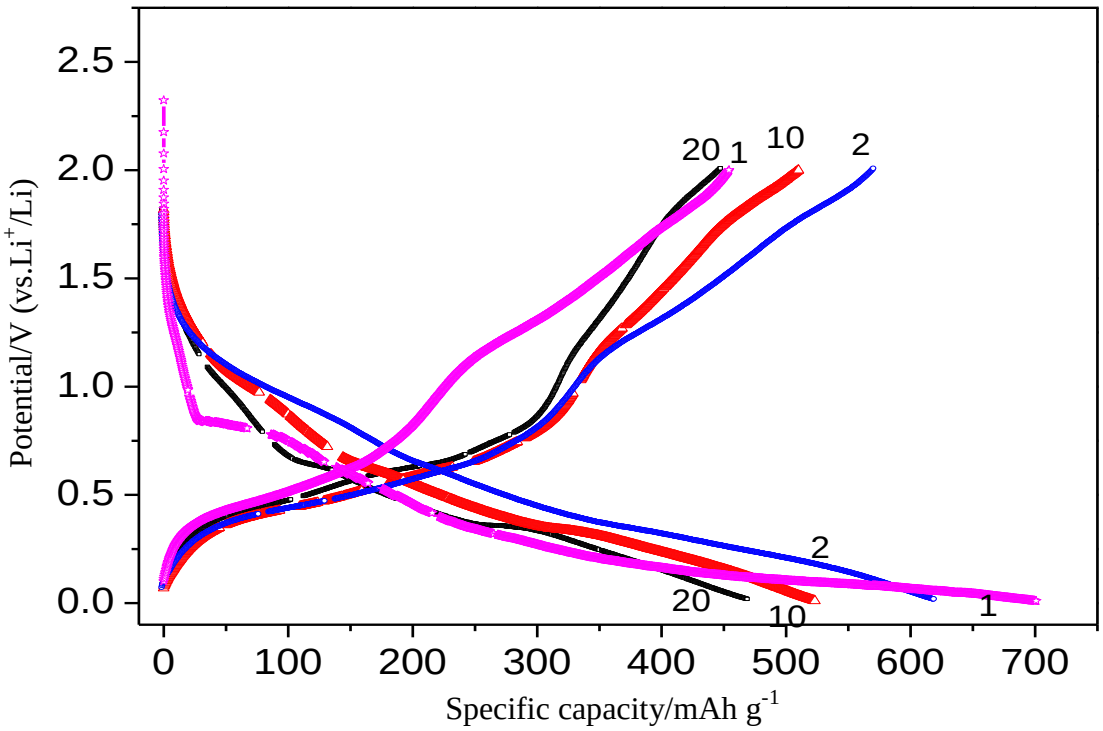

Figure 3. The charge/discharge curves of the the Sn-Ni alloy composite

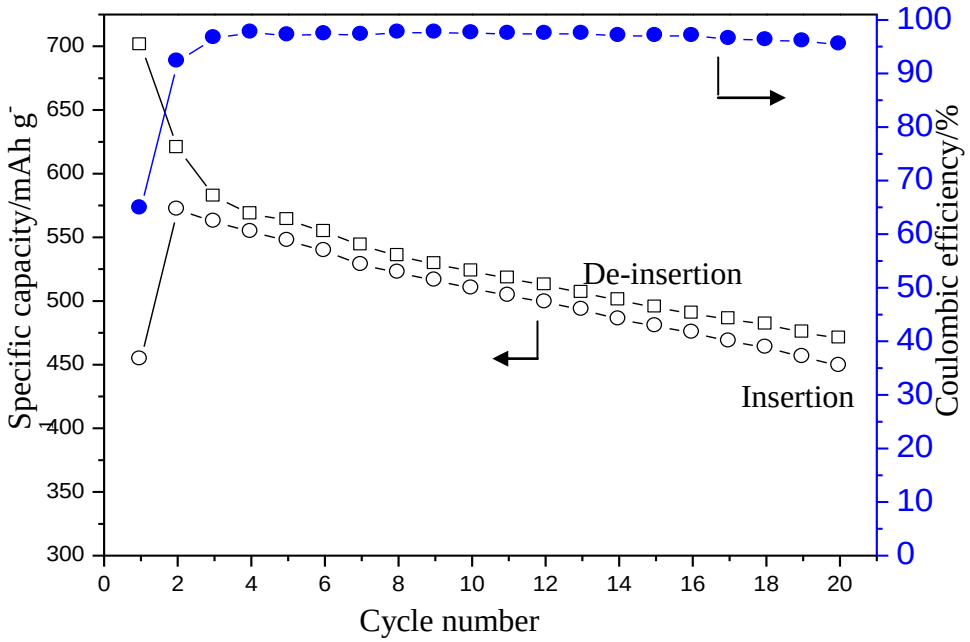

Figure 4. Cycling performance of the Sn-Ni alloy composite

The plot also showed that the alloy composite shows a first lithium de-insertion capacity of 454.1mAh/g and increased to 571.1 mAh/g at the second cycle. The latter is about 98.1% of the theoretical capacity of the Sn-Ni alloy composite thus prepared (582 mAh/g). The lower value of the first cycle is ascribed to the "active" of the alloy and forms the amorphous state. Thus the first cycle shows a relative lower insertion potential and a relative higher de-insertion potential in compared with the following cycles shown in figure 3.

The cycling performance of the sample is shown in figure 4. It showed that the highest reversible capacity of alloy composite was 571.1 mAh/g at the second cycle. The reversible capacity at the 20^{th} is 448.9 mAh/g, which is about the same value of the first cycle and 78.6% of the second cycle. The improved cycling performance was ascribed to the decreased of the particle size, the higher contents of alloy phase, the binder SBR and CMC to buffer the expansion of the alloy.

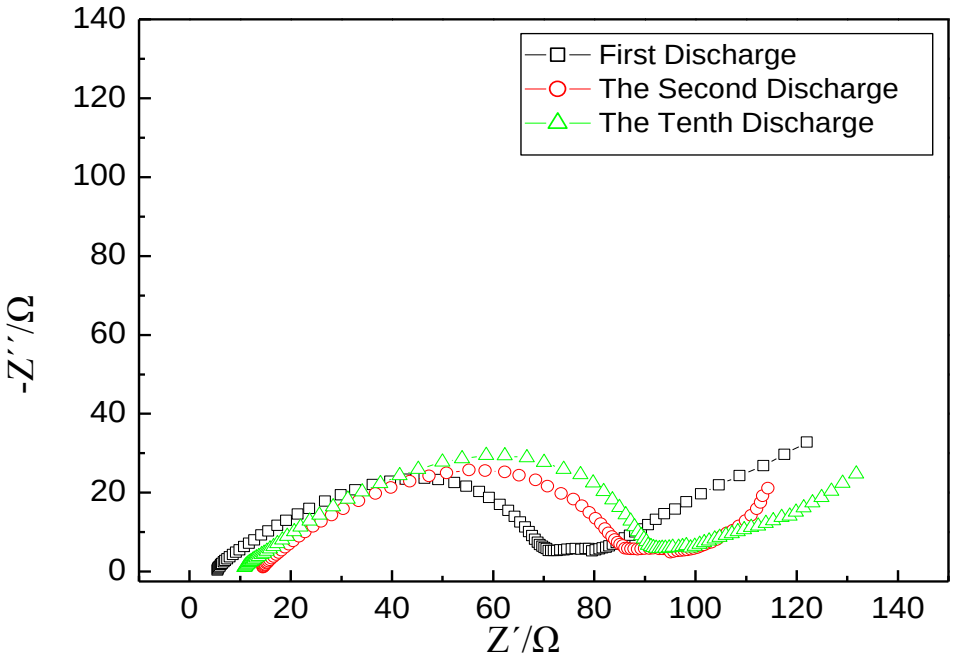

Figure 5. Typical EIS of the Sn-Ni alloy composite after different charge/discharge cycles

The EIS of the alloy composite electrode after different times of discharge test are shown in figure 5. The plot showed that the diameter of the first semicircle was increased with cycles. It is generally ascribed the first semicircle to the SEI formation and the increase of the diameter means that the impedance was increased with charge/discharge cycles due to the pulverization of alloy during the charge/discharges cycles. The pulverization results the new surface and the reduction of the electrolyte to form SEI on the newly formed surface. Furthermore, the pulverization also results in the destruction of the origin SEI and the repairing of the SEI results in the increase of the thickness of SEI, which is similar to that occurred on the surface of graphite [25]. The EIS also showed that the contact resistance was increased after first discharge, which may be come from the decrease of the electrical contact between copper current collector and Sn-Ni active material after charge/discharge cycles due to the

volume expansion of alloy during the lithium insertion process. But the contact resistances of the second and the tenth discharge were almost the same means that this decrease was mainly occurred during the first lithium insertion process. The good electric contact between active material and copper current collector is another reason that improves the cyclic stability of the alloy composite prepared in this paper.

4. CONCLUSIONS

The Sn-Ni alloy composite as the anode for lithium ion battery has been synthesized by carbothermal reduction of SnO_2, NiO at 900 ^oC with ball-milling and spray drying to obtain the precursor. The alloy shows a spherical-like morphology with a diameter below 200 nm. The alloy shows a reversible capacity of 571.1 mAh/g and a capacity retention of 78.4% after 20 cycles. The improved performance was ascribed to the lower particle size, the higher alloy phase contents, the binder SBR and CMC to buffer the expansion of the alloy and the improved electric contact between active material and copper current collector.

ACKNOWLEDGEMENT
The financial support from the National Natural Science Foundation of China (No. 20903014), Doctoral Fund of Shandong Province (No. BS2010CL001) and Binzhou University (No. 2008Y01, No. 2008ZDL04) will be greatly appreciated.

References

1. M. Winter, J. O. Besenhard, *Electrochim. Acta*, 45 (1999) 31
2. W.-J Zhang, *J. Power Sources*, 196 (2011) 13
3. http://www.sony.net/SonyInfo/News/Press/200502/05-006E/
4. O. Crosnier, T. Brousse, X. Devaux, P. Fragnaud, D.M. Schleich, *J. Power Sources*, 94 (2001) 169
5. H. Mukaibo, T. Momma, T. Osaka, *J. Power Sources*, 146 (2005) 457
6. J. Hassoun, S. Panero, B. Scrosati, *J. Power Sources*, 160 (2006) 1336.
7. L. Huang, H.-B.Wei, F.-S. Ke, X.-Y. Fan, J.-T. Li, S.-G. Sun, *Electrochim. Acta*, 54 (2009) 2693
8. J. Hassoun, S. Panero, P. Reale and B. Scrosati, *Int. J. Electrochem. Sci.*, 1 (2006) 110
9. J.-J Zhang, Y.-M Zhang, X. Zhang, Y.-Y. Xia, *J. Power Sources*, 167 (2007) 171
10. X.-Q. Cheng, P.-F. Shi, *J. Alloys and Compd.*, 391 (2005) 241
11. H. Guo, S. Zhao, H. Zhao, Y. Chen, *Electrochim. Acta*, 54 (2009) 4040
12. H. Guo, H. Zhao, X. Jia, *Electrochem. Comm.*, 9 (2007) 2207
13. F. Nobili, S. Dsoke, T. Mecozzi, R. Marassi, *Electrochim. Acta*, 51 (2005) 536
14. J.H. Ahn, G.X. Wang, J. Yao, H.K. Liu, S.X. Dou, *J. Power Sources*, 119–121 (2003) 45
15. A.B. D. Nandiyanto, K. Okuyama, *Adv. Powder Technol.*, 22 (2011) 1
16. S. H. Ju, H. C. Jang, Y. C. Kang, D.-W. Kim, *J. Alloys and Compd.*, 478 (2009) 177
17. B. Huang, X.D. Zheng, D.M Jia, M.Lu, *Electrochim. Acta*, 55 (2010) 1227
18. O. Crosnier, T. Brousse, X. Devaux, P. Fragnaud, D.M. Schleich, *J. Power Sources*, 94 (2001) 169
19. L.G Xue, Z.H. Fu, Y. Yao, T. Huang, A.S. Yu, *Electrochim. Acta*, 55 (2010) 7310
20. H. Guo, X.-F. Lin, Y.-S. Chen, *Trans.Nonferrous Met.Soc.China*, 20 (2010) s253

21. Y.-X. Wang, L. Huang, Y.-Q. Chang, F.-S. Ke, J.-T. Li, S.-G. Sun, *Electrochem. Comm.*, 12 (2010) 1226
22. J.-J. Zhang, Y.-M. Zhang, X. Zhang, Y.-Y. Xia, *J. Power Sources*, 167 (2007) 171
23. F. D. Lupo, C. Gerbaldi, G. Meligrana, S. Bodoardo, N. Penazzi, *Int. J. Electrochem. Sci.*, 6 (2011) 3580
24. S. Ohara, J. Suzuki, K. Sekine, T. Takamura, *J. Power Sources*, 136 (2004) 303
25. M. Lu, H. Cheng, Y. Yang, *Electrochim. Acta*, 53 (2008) 3539